Biophysical Reports

LETTER

Separation of spectrally overlapping fluorophores using intra-exposure excitation modulation

Hana Valenta,[1] Siewert Hugelier,[1] Sam Duwé,[2] Giulia Lo Gerfo,[3] Marcel Müller,[4] Peter Dedecker,[1,*] and Wim Vandenberg[1,*]

[1]Laboratory for Nanobiology, Department of Chemistry, KU Leuven, Leuven, Belgium; [2]Advanced Optical Microscopy Centre, Hasselt University, Hasselt, Belgium; [3]Molecular Nanophotonics, ICFO, Barcelona, Spain; and [4]Faculty of Physics, Bielefeld University, Bielefeld, Germany

ABSTRACT Multicolor fluorescence imaging is an excellent method for the simultaneous visualization of multiple structures, although it is limited by the available spectral window. More labels can be measured by distinguishing these on properties, such as their fluorescence dynamics, but usually these dynamics must be directly resolvable by the instrument. We propose an approach to distinguish emitters over a much broader range of light-induced dynamics by combining fast modulation of the light source with the detection of the time-integrated fluorescence. We demonstrate our method by distinguishing four spectrally overlapping photochromic fluorophores within *Escherichia coli* bacteria, showing that we can accurately classify all four probes by acquiring just two to four fluorescence images. Our strategy expands the range of probes and processes that can be used for fluorescence multiplexing.

WHY IT MATTERS The simultaneous measurement of multiple components is essential to understand complex systems. Fluorescence microscopy readily allows this, but more information can be measured if the labels are also distinguished on properties other than their emission color. We introduce an approach to distinguish fluorophores based on the characteristic light-induced fluctuations in their fluorescence emission. Our method does not require that these fluctuations are resolvable with the imaging instrument, only that the excitation light can be modulated on a similar timescale, making it compatible with a very broad range of temporal dynamics. Overall, we anticipate that our method provides a widely applicable approach for the separation and classification of spectrally overlapping fluorophores.

INTRODUCTION

A key advantage of fluorescence microscopy is the availability of labels with different colors, making it possible to measure multiple targets via multicolor imaging. However, the number of labels that can be multiplexed in this way is limited by the extent of the spectral window. The need to visualize multiple targets is becoming increasingly important as more and more investigations move to high-content imaging because this provides increased opportunities to understand complex processes.

One way to measure more types of labels is to separate these on properties other than their excitation and emission spectra, such as their excited-state lifetimes (1–5) or fluorescence anisotropy (6). Alternatively, one can distinguish labels based on light-induced processes that result in characteristic temporal dynamics in the emission. A number of such methods have previously been demonstrated, including optical lock-in detection (7–9), out-of-phase imaging after optical modulation (10,11), synchronously amplified fluorescence image recovery (12), multiple τ photochromic superresolution optical fluctuation imaging (13), and approaches based on photobleaching and fluorescence recovery (14,15).

These methods require that the dynamics lie within the temporal resolution of the system. In widefield instruments, this resolution is limited by the exposure and readout time of the camera, usually in the tens to hundreds of milliseconds range. However, even inexpensive light sources can now be rapidly modulated within timescales ranging from micro- to nanoseconds, suggesting

Submitted July 18, 2021, and accepted for publication September 17, 2021.

*Correspondence: peter.dedecker@kuleuven.be or wim.vandenberg@kuleuven.be

Hana Valenta and Siewert Hugelier contributed equally to this work.

Sam Duwé's present address is Advanced Optical Microscopy Centre, Hasselt University, Hasselt, Belgium.

Giulia Lo Gerfo's present address is Molecular Nanophotonics, ICFO, Barcelona, Spain.

Marcel Müller's present address is Faculty of Physics, Bielefeld University, Bielefeld, Germany.

Editor: Jorg Enderlein.

https://doi.org/10.1016/j.bpr.2021.100026

TABLE 1 Sequence of illumination pulses for one cycle consisting of four fluorescence images. Due to the rolling shutter readout process, the 50 ms camera exposure resulted in a per-image illumination duration of 40 ms because light was applied only when all of the camera pixels were sensitive

Image	Cyan illumination duration (ms)	Number of violet activation pulses	Violet pulse duration (ms)
1	40	1	3
2	40	0	NA
3	40	3	1.5
4	40	1	40

that a much broader range of fluorescence dynamics could be probed if one could examine these using only such modulation. An analogous concept was previously introduced in transient state spectroscopy (16), in which the microsecond-range blinking of a dye was probed by exciting it with rapidly modulated excitation light. Even though the much slower detector could not resolve these dynamics directly, the kinetics of the blinking could be determined by measuring the integrated fluorescence over a range of excitation patterns. This method has since been demonstrated both for solution measurements (17,18) and live cell studies (19,20).

We reasoned that a conceptually related approach could be used to distinguish fluorophores that show distinct light-inducible dynamics, even when these occur too quickly to be resolved directly. Such an approach could not only expand the range of dynamics that can be addressed but could also provide considerably faster imaging by not requiring the use of slower processes.

One way to provide these dynamics is to make use of photochromic fluorophores, which display light-induced "on-off" switching of the fluorescence, including a broad range of fluorescent proteins (21–25). In photochromic green fluorescent proteins, for example, cyan light simultaneously induces fluorescence emission and conversion to a nonfluorescent state, which can then be recovered by illumination with violet light. This switching can occur on very short timescales (26), and a broad range of proteins with different sensitivities to the on- and off-switching light is available or can be generated (27).

In this contribution, we develop a strategy to distinguish fluorophores based on their light-induced dynamics by acquiring a few fluorescence images in which the excitation light is rapidly modulated and detecting only the time-integrated fluorescence. We apply our method to resolve mixtures of bacteria, each expressing one of four fluorophores, showing that very good classification of each fluorophore is possible when acquiring just two to four fluorescence images in total. We expect that this approach can be applied to any fluorophore that shows characteristic light-induced dynamics, as it is limited only by the rate at which the light sources can be modulated.

MATERIALS AND METHODS

Cell preparation for imaging

Escherichia coli JM109 cells were transformed with pRSETb expression vectors. A single colony was used to set a 4 mL overnight culture in Luria-Bertani (LB) medium (Sigma-Aldrich, Burlington, MA), which was diluted the next morning and grown at 37°C until the optical density $(OD)_{600}$ reached 0.6. The cells were then centrifuged, washed three times with Hanks' Balanced Salt Solution (Thermo Fisher Scientific, Schiphol, the Netherlands), and resuspended in 100 μLof the same buffer. 4 μL was deposited on a coverslip covered with 2% agarose (VWR Chemicals, Aurora, Ohio) pads, and a 1.5 mm slide glass coated with poly-L-lysine (Sigma-Aldrich) was put on top immediately after.

Fluorescence intensity decays measurement

The measurements shown in Fig. 2 were performed using an Olympus IX71 (Olympus, Tokyo, Japan) inverted microscope equipped with a SPECTRA X light engine (Lumencor, Beaverton, Oregon), an UMPlanFI 50×/0.80 BD objective (Olympus, Tokyo, Japan), and a ZT488RDC dichroic mirror and ET525/30m emission filter (both Chroma Technology, Bellows Falls, Vermont). The cyan (485/25×) and violet (390/22×) channels were used for excitation, with total light powers (measured by a Thorlabs PM100D power meter with a S170C detector (Dachau, Germany) of ∼1.4 and 7.7 mW transmitted by the objective. Images were acquired on an ORCA-Flash4.0 LT+ camera (Hamamatsu Photonics, Hamamatsu City, Japan) with an exposure time of 2.5 ms.

Widefield image acquisition

Imaging was performed on a Nikon Eclipse Ti-2 Inverted Microscope (Minato City, Japan) equipped with a 1.4 NA oil immersion objective (×100 CFI Apochromat Total Internal Reflection Fluorescence) and a ZT405/488/561/640rpcv2 dichroic mirror with a ZET405/488/561/640 m emission filter (both Chroma Technology, Bellows Falls, Vermont) in epi-illumination. We also added an neutral density 2.0 filter to the emission path to prevent saturation of the detector by the fluorescence emitted from the very highly expressing bacteria. We applied this strategy because reducing the excitation light would slow down the kinetics of the photochromism. Two separate lasers at 405 and 488 nm (Oxxius, Lannion, France) were used for excitation. Images were acquired on a pco.edge 4.2 camera (PCO, Kelheim, Germany) with an exposure time of 50 ms and optical pixel size of78.8 nm, using varying pulses of the 405 nm light (∼11 mW transmitted by the objective) in the presence of 488 nm light (∼10 mW transmitted by the objective) (Table 1). The excitation light was controlled using an Arduino-compatible microcontroller (Velleman, Gavere, Belgium). 35 different fields-of-view were recorded for each measurement.

Image analysis

The homemade analysis routine consists of four different parts that were written in MATLAB R2018b (The MathWorks, Natick, MA). The full source code and representative experimental data are available online at https://doi.org/10.5281/zenodo.5500306.

Background removal

The first step is to subtract uniform background from the images. Given the N pixels present in the fluorescence image, the set of

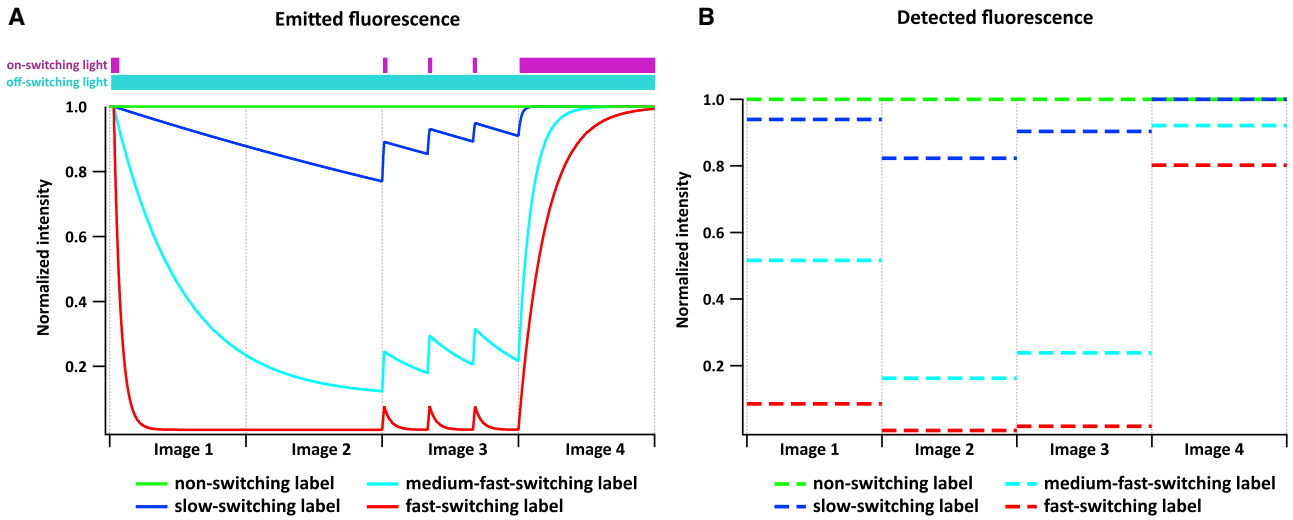

FIGURE 1 Concept of the strategy. (*A*) Spectrally indistinguishable photochromic labels with different on- and off-switching efficiencies are exposed to quickly varying illumination patterns. (*B*) The camera detector measures the integrated fluorescence over each pattern, leading to a distinct intensity profile for each of the labels.

background pixels was defined by selecting all pixels with a value lower than 10.5*m*, where *m* is the value of the lowest-intensity pixel in the image. If the number of background pixels defined in this manner is smaller than $\sqrt{N}$ (i.e., 1024 in our case), the threshold value is progressively multiplied by 1.05 until this condition is met. The background signal is then estimated as theaverage of these pixels.

Image segmentation

To segment the bacteria, we applied a two-step algorithm. In the first step, we applied a global threshold with a cutoff value of 50% of the mean signal, which was then followed by filling in imperfections and removing small objects (<50 pixels). The resulting mask fromthis first step was then subjected to an edge detection algorithm based on the Laplacian of the Gaussian method (28), after which we corrected again for imperfections and small objects. Additionally, round objects were also removed to select only apparently healthy bacteria.

Signal extraction

The fluorescence signals are extracted by taking the average of all pixels assigned to a single bacteria. Bacteria for which more than one-tenth of the pixel values were within 5% of the saturation value of the camera were removed. The intensity trajectory of each bacterium was normalized to the fluorescence intensity observed in the fourth image.

Classification

We then classified the bacteria based on their response to illumination. We used k-means clustering in a three-dimensional space consisting of the intensities observed in the first three images (all normalized to the fourth image). In this unsupervised method, the data set is iteratively divided into distinct clusters, without reference to any control experiments other than to identify the fluorophores associated with the final centroids. Bacteria expressing an unknown fluorophore are then assigned to the nearest cluster centroid. Applying this method on pure samples allowed us to obtain confusion matrices representing the sensitivity and specificity of the classification.

To evaluate the robustness of our method, the same approach was also explored in a two-dimensional (considering only the normalized fluorescence intensities observed in the first two images) and one-dimensional space (considering the normalized fluorescence intensity observed in the first image).

RESULTS AND DISCUSSION

Fig. 1 shows the concept underlying our approach. We assume that the sample is labeled with photochromic fluorophores that show different photochromism rates when exposed to the same illumination intensities. This sample is imaged using a widefield instrument that contains two different light sources capable of triggering the photochromism. In particular, with the photochromic green fluorescent proteins used here, cyan light causes fluorescence emission and off-switching, whereas the violet light induces the recovery of the fluorescent state.

We reasoned that the dynamics of the photochromism should also be evident when the activation light is rapidly modulated, even if only the integrated fluorescence on a (much) longer timescale is observed. Indeed, as shown in Fig. 1, the combination of the different photochromism efficiencies and excitation patterns can be used to obtain a different and characteristic fluorescence response for each type of fluorophore, suggesting that this approach could be used to distinguish these labels experimentally.

We selected four photochromic green fluorescent proteins to evaluate this approach: EGFP (29), ffDronpa (30), ffDronpaF (ffDronpa K45I/F173V (13)), and ffDronpa2F (ffDronpa K45I/M159T/F173V). All four have very similar spectra (absorption and emission maxima: EGFP 488/507 nm, ffDronpa and ffDronpaF 503/518 nm, ffDronpa2F 486/510 nm), but show pronounced differences in their photochromism

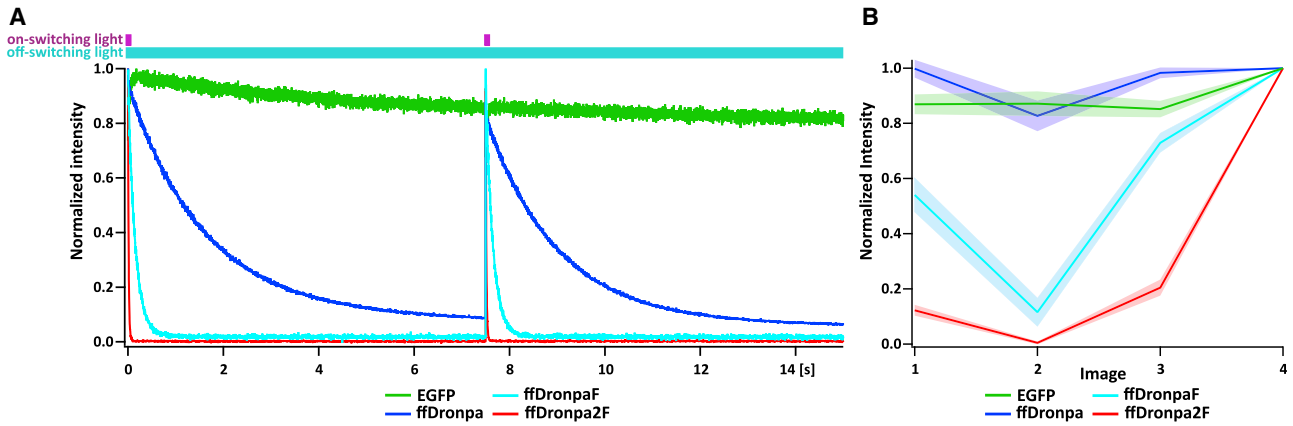

FIGURE 2 Characterization of photoswitching dynamics of four green fluorescent proteins expressed in *E.coli*. (*A*) Normalized fluorescence intensity decays of two cycles. (*B*) Normalized fluorescence intensity traces of FPs when exposed to the irradiation sequence shown in Fig. 1 *A* (*shaded region* represents the standard deviations).

efficiency. To verify this, we first conducted characterization measurements on *E. coli* cells transformed with plasmids encoding the different fluorophores. Fast measurements using a small region of interest indeed showed very different switching kinetics when exposed to the same illumination intensities (Fig. 2 *A*).

We then examined whether these labels showed characteristic responses using our modulation scheme on a different microscope that was capable of higher illumination intensities. We applied the measurement and irradiation sequence shown in Fig. 1, which resulted in distinct intensity trajectories for the detected time-integrated fluorescence (Fig. 2 *B*), suggesting that these could indeed be used to identify the different labels experimentally.

We next applied our scheme to samples consisting of mixtures of bacteria separately transformed with the different plasmids and applied the analysis methodology described in Materials and methods. As we show in Fig. 3, *A* and *B*, the different fluorophores could indeed be readily and reliably identified, allowing us to rapidly classify the different bacteria by acquiring just four fluorescence images, as is also confirmed by visual inspection of the intensities recorded in these images (Fig. 3 *C*). As can also be seen in Fig. 3, it was impossible to use only the fluorescence brightness to distinguish the bacteria expressing different fluorescent proteins (FPs).

Verification using confusion matrices (Fig. 3 *D*) showed that our method performs an essentially perfect classification in samples consisting of just a single fluorescent protein. We did observe that the separation was slightly less clear on the mixed samples (Fig. 3 *C*), presumably because of light scattering in the sample and/or out-of-focus fluorescence, so that the classification of the mixture is likely slightly worse than that predicted by these numbers. Overall, these data show that our approach can readily discern light-induced processes that occur beyond the overall temporal resolution of the instrument, limited only by the rate at which the excitation light can be modulated.

We next determined whether we could perform the same classification using fewer acquired images. A similar analysis based on confusion matrices found that the use of three different fluorescence images was sufficient to classify the bacteria with essentially perfect accuracy and that two fluorescence images could be used for a less powerful but still highly accurate analysis (Fig. 3 *D*). This shows that our method could be used to classify fluorophores within a very short acquisition time.

CONCLUSIONS

We have presented a general way to distinguish fluorophores based on their light-induced fluorescence dynamics. Compared with other approaches, our method requires only the fast modulation of the excitation light and the detection of the time-integrated fluorescence. This expands the range of fluorophores that can be distinguished by not requiring that their dynamics are observable within the temporal resolution of the instrument.

We demonstrated our strategy by classifying fluorescent bacteria according to which one of four photochromic fluorescent proteins they expressed. In principle, our method is not restricted to the use of photochromic labels. It could also be used with labels that undergo light-induced conversion followed by spontaneous recovery, as long as the characteristic timescales for the dynamics are sufficiently well separated.

Although the quantitative separation of mixtures of four probes, which we did not consider here, does

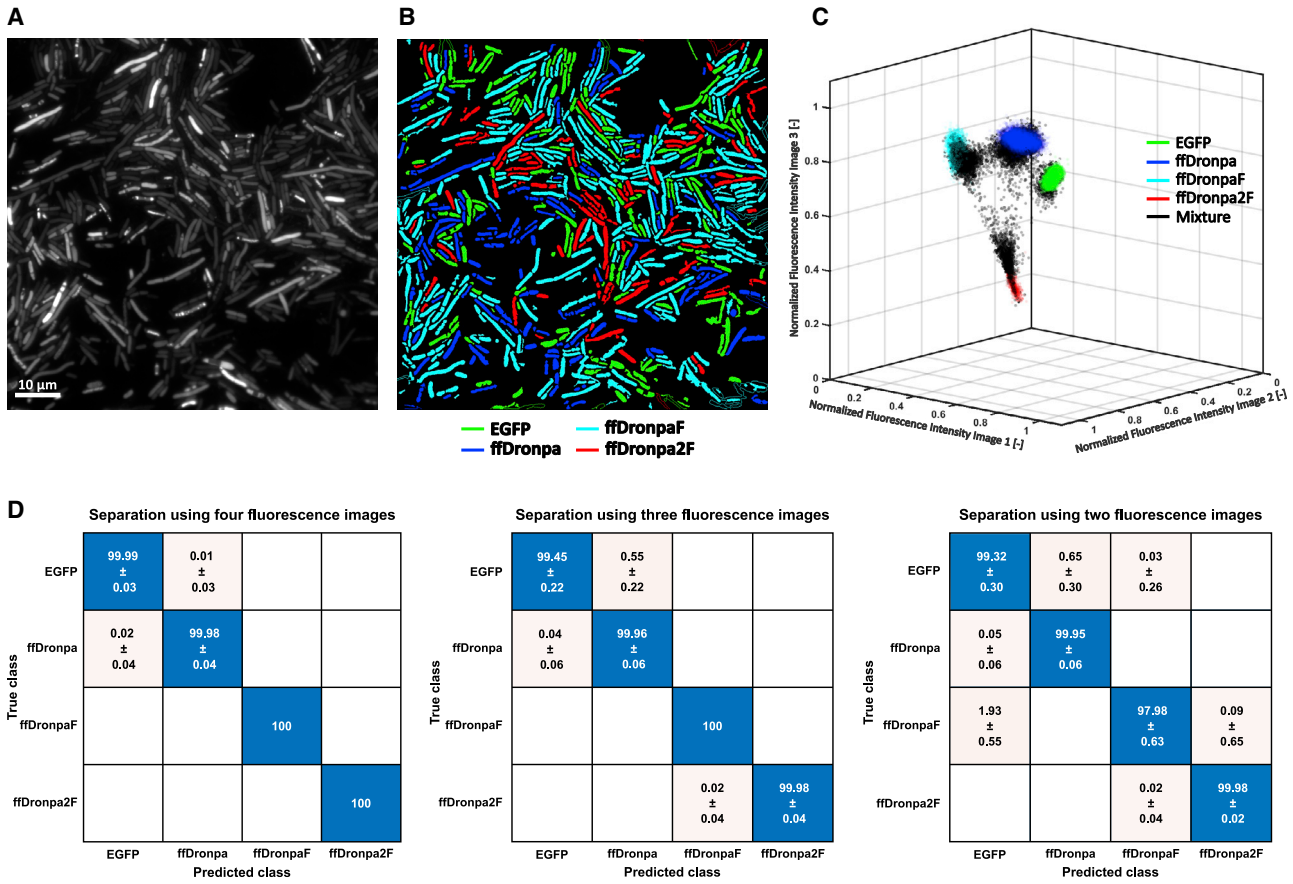

FIGURE 3 Separation of four green FPs expressed in *E. coli*. (*A*) Fluorescence image of transformed bacteria. (*B*) False color image of separated proteins. (*C*) Visualization of the bacterial fluorescence intensities observed in the first three fluorescence images, normalized to the intensity of the fourth image. The different colors show bacteria expressing only the indicated label and a mixture of such bacteria. (n_{EGFP}= 8516, $n_{ffDro_{np}a}$ = 10,801, $n_{ffDronpaF}$ = 14,898, $n_{ffDronpa2F}$ = 6249, and $n_{Mixture}$ = 9378). (*D*) Confusion matrices showing the accuracy of the separation algorithm using four, three, and two fluorescence images (expressed as percentage).

indeed require the acquisition of four different fluorescence images, the conceptually simpler classification of objects expressing just one label can be done using fewer measurements. In particular, we showed that two or three fluorescence images were enough to perform this classification with very good accuracy.

In summary, we have presented a new, to our knowledge, approach for the separation of fluorophores based on their intrinsic fluorescence dynamics. By relying on the fast on-off modulation of the excitation light and the detection of the integrated fluorescence intensity, this method is compatible with a very broad range of temporal dynamics. Overall, we anticipate that our method provides a widely applicable approach for the separation and classification of spectrally overlapping fluorophores.

AUTHOR CONTRIBUTIONS

W.V., P.D., and M.M. designed research. M.M. designed and implemented the instrument control. S.H. designed and implemented the data analysis. W.V., P.D., H.V., and S.H. designed experiments. H.V., S.H., and W.V. performed classification experiments. H.V., G.L.G., and W.V. performed characterization experiments. H.V. and S.H. analyzed data. P.D., H.V., S.H., and W.V. wrote the manuscript with input from all authors.

DECLARATION OF INTERESTS

The authors declare no competing interests.

ACKNOWLEDGMENTS

We thank Viola Mönkemöller for supporting initial experiments and analysis related to this work. Siewert Hugelier and Sam Duwé thank the Research Foundation - Flanders (FWO) for a postdoctoral fellowship.

This work was supported through funding from the FWO, through grants G090819N and G0B8817N; the European Research Council, through grant 714688 NanoCellActivity; and the Katholieke Universiteit Leuven, through grant C14/17/111. This project also received funding from the European Union's Horizon 2020 research and innovation programme under the Marie Skłodowska-Curie grant agreement No. 752080.

REFERENCES

1. Bückers, J., D. Wildanger, …, S. W. Hell. 2011. Simultaneous multi-lifetime multi-color STED imaging for colocalization analyses. *Opt. Express.* 19:3130–3143.
2. Kremers, G.-J., E. B. van Munster, …, T. W. Gadella, Jr. 2008. Quantitative lifetime unmixing of multiexponentially decaying fluorophores using single-frequency fluorescence lifetime imaging microscopy. *Biophys. J.* 95:378–389.
3. Schlachter, S., S. Schwedler, …, C. F. Kaminski. 2009. A method to unmix multiple fluorophores in microscopy images with minimal a priori information. *Opt. Express.* 17:22747–22760.
4. Fereidouni, F., G. A. Blab, and H. C. Gerritsen. 2013. Blind unmixing of spectrally resolved lifetime images. *J. Biomed. Opt.* 18:86006.
5. Niehörster, T., A. Löschberger, …, M. Sauer. 2016. Multi-target spectrally resolved fluorescence lifetime imaging microscopy. *Nat. Methods.* 13:257–262.
6. Testa, I., A. Schönle, …, A. Egner. 2008. Nanoscale separation of molecular species based on their rotational mobility. *Opt. Express.* 16:21093–21104.
7. Marriott, G., S. Mao, …, Y. Yan. 2008. Optical lock-in detection imaging microscopy for contrast-enhanced imaging in living cells. *Proc. Natl. Acad. Sci. USA.* 105:17789–17794.
8. Yan, Y., M. E. Marriott, …, G. Marriott. 2011. Optical switch probes and optical lock-in detection (OLID) imaging microscopy: high-contrast fluorescence imaging within living systems. *Biochem. J.* 433:411–422.
9. Abbandonato, G., B. Storti, …, R. Bizzarri. 2016. Quantitative optical lock-in detection for quantitative imaging of switchable and non-switchable components. *Microsc. Res. Tech.* 79:929–937.
10. Querard, J., T.-Z. Markus, …, L. Jullien. 2015. Photoswitching kinetics and phase-sensitive detection add discriminative dimensions for selective fluorescence imaging. *Angew. Chem. Int. Ed. Engl.* 54:2633–2637.
11. Quérard, J., R. Zhang, …, L. Jullien. 2017. Resonant out-of-phase fluorescence microscopy and remote imaging overcome spectral limitations. *Nat. Commun.* 8:969.
12. Hsiang, J.-C., A. E. Jablonski, and R. M. Dickson. 2014. Optically modulated fluorescence bioimaging: visualizing obscured fluorophores in high background. *Acc. Chem. Res.* 47:1545–1554.
13. Duwé, S., W. Vandenberg, and P. Dedecker. 2017. Live-cell monochromatic dual-label sub-diffraction microscopy by mt-pcSOFI. *Chem. Commun. (Camb.).* 53:7242–7245.
14. Brakenhoff, G. J., K. Visscher, and E. J. Gijsbers. 1994. Fluorescence bleach rate imaging. *J. Microsc.* 175:154–161.
15. Hugelier, S., R. Van den Eynde, …, P. Dedecker. 2021. Fluorophore unmixing based on bleaching and recovery kinetics using MCR-ALS. *Talanta.* 226:122117.
16. Sandén, T., G. Persson, …, J. Widengren. 2007. Monitoring kinetics of highly environment sensitive states of fluorescent molecules by modulated excitation and time-averaged fluorescence intensity recording. *Anal. Chem.* 79:3330–3341.
17. Sandén, T., G. Persson, and J. Widengren. 2008. Transient state imaging for microenvironmental monitoring by laser scanning microscopy. *Anal. Chem.* 80:9589–9596.
18. Hevekerl, H., J. Tornmalm, and J. Widengren. 2016. Fluorescence-based characterization of non-fluorescent transient states of tryptophan - prospects for protein conformation and interaction studies. *Sci. Rep.* 6:35052.
19. Spielmann, T., L. Xu, …, J. Widengren. 2014. Transient state microscopy probes patterns of altered oxygen consumption in cancer cells. *FEBS J.* 281:1317–1332.
20. Chmyrov, V., T. Spielmann, …, J. Widengren. 2015. Trans-cis isomerization of lipophilic dyes probing membrane microviscosity in biological membranes and in live cells. *Anal. Chem.* 87:5690–5697.
21. Bourgeois, D., and V. Adam. 2012. Reversible photoswitching in fluorescent proteins: a mechanistic view. *IUBMB Life.* 64:482–491.
22. Dedecker, P., F. C. De Schryver, and J. Hofkens. 2013. Fluorescent proteins: shine on, you crazy diamond. *J. Am. Chem. Soc.* 135:2387–2402.
23. Roebroek, T., S. Duwé, …, P. Dedecker. 2017. Reduced fluorescent protein switching fatigue by binding-induced emissive state stabilization. *Int. J. Mol. Sci.* 18:2015.
24. Rodriguez, E. A., R. E. Campbell, …, R. Y. Tsien. 2017. The growing and glowing toolbox of fluorescent and photoactive proteins. *Trends Biochem. Sci.* 42:111–129.
25. Roebroek, T., W. Vandenberg, …, P. Dedecker. 2021. Simultaneous readout of multiple FRET pairs using photochromism. *Nat. Commun.* 12:2005.
26. Dedecker, P., J. Hotta, …, J. Hofkens. 2006. Fast and reversible photoswitching of the fluorescent protein dronpa as evidenced by fluorescence correlation spectroscopy. *Biophys. J.* 91:L45–L47.
27. De Zitter, E., S. Hugelier, …, P. Dedecker. 2021. Structure-function dataset reveals environment effects within a fluorescent protein model system*. *Angew. Chem. Int. Ed. Engl.* 60:10073–10081.
28. Sotak, G., and K. Boyer. 1989. The Laplacian-of-Gaussian kernel: a formal analysis and design procedure for fast, accurate convolution and full-frame output. *Comput. Vis. Graph. Image Process.* 48:147–189.
29. Cormack, B. P., R. H. Valdivia, and S. Falkow. 1996. FACS-optimized mutants of the green fluorescent protein (GFP). *Gene.* 173:33–38.
30. Moeyaert, B., N. Nguyen Bich, …, P. Dedecker. 2014. Green-to-red photoconvertible Dronpa mutant for multimodal super-resolution fluorescence microscopy. *ACS Nano.* 8:1664–1673.